NUMERICAL SIMULATION OF THE PLASTIC DEBRIS TRANSPORT IN NEARSHORE ZONE

Claudio Iuppa[1*] and Carla Faraci[1]

Plastic is a vital material for both our economy and daily life. However, it can have significant negative impacts on environmental health. For this reason, extensive research has been dedicated to studying plastic behaviour in various natural environments. In the marine environment, research activities are typically divided into studies focusing on either the offshore zone (deep water) or the nearshore zone (intermediate and shallow water). Offshore studies often rely on numerical models, which are relatively effective in predicting plastic transport. In contrast, numerical models for intermediate and shallow waters are still at the early stages of development. This limitation stems from the need for nearshore models to simulate near-bed phenomena accurately, particularly when studying the dynamics of non-floating plastics. Currently, researchers at the University of Messina are developing numerical models to predict the behaviour of plastic debris in coastal zones. The developed model, called TRANMPD-HM, is based on XBeach, with several modifications introduced to evaluate the effects of waves and currents on plastic dynamics. To validate the effectiveness of these modifications, a comparison was made with data from an experimental campaign conducted on various types of plastics. The results confirmed that the changes introduced enable the simulation of plastic transport under the influence of wave action with a high degree of reliability.

Keywords: Plastic debris transport; Xbeach; Nearshore zone

INTRODUCTION

The increasing accumulation of plastic debris in coastal waters has emerged as a significant environmental challenge over recent decades. This issue is particularly critical in nearshore zones, where the highest concentrations of plastic waste, especially at the sea bottom, in the case of non-buoyant plastics, are observed due to the complex interplay of waves, currents, and seabed morphology (Forsberg et al., 2020; Alsina et al., 2020).

Understanding the mechanisms governing the transport and fate of plastics is essential for mitigating their environmental impact and informing effective management strategies. While numerical models have been widely used to simulate plastic transport at large scales, predicting the dynamics at nearshore scales, dominated by wave-induced hydrodynamics, remains a challenge (Liubartseva et al., 2018; Guerrini et al., 2021).

Recently, several laboratory studies have been conducted to investigate the dynamics of plastic transport under controlled conditions. For instance, Forsberg et al. (2020) analysed the cross-shore distribution of plastic particles in a wave flume under regular wave and wind conditions, highlighting the importance of density and particle shape. Alsina et al. (2020) studied the transport of buoyant and non-buoyant particles under regular waves, demonstrating how wave steepness influences particle velocity. Guler et al. (2022) investigated the transport of non-buoyant microplastics under breaking irregular waves on a mobile sediment bed, examining the interplay between hydrodynamic forces and sediment dynamics, with a focus on the influence of wave breaking, sediment characteristics, and microplastic properties on transport patterns. Núñez et al. (2023) explored the effects of regular and irregular wave regimes on plastic dispersion in the nearshore zone, focusing on accumulation patterns relative to particle buoyancy and wave characteristics. The research carried out by Iuppa et al. (2024) examines the behaviour of different plastic types under a range of hydrodynamic conditions driven predominantly by wave action. Over 200 scenarios were tested, varying wave properties, water depth, plastic debris characteristics (including density and shape), and the roughness of the fixed seabed. These experimental efforts provide valuable benchmarks for the calibration and validation of numerical models aimed at predicting plastic transport in coastal environments.

This study focuses on calibrating a numerical model to predict plastic transport driven by wave action, considering the effects of particle density and shape aiming to bridge the gap between empirical observations and numerical predictions. The work described here focuses on implementing a module dedicated to simulating non-buoyant micro-plastic debris (TRANMPD) transport within a hydro-morphodynamic (HM) numerical model (Iuppa and Faraci, 2024). The proposed model is a modified version of XBeach, an open-source numerical model widely used to simulate hydrodynamic effects on coastal morphodynamics and sediment transport processes (Roelvink et al., 2018).

[1]Department of Engineering, University of Messina, Italy. Corrisponding author: claudio.iuppa@unime.it

The paper is organized as follows: Chapter 2 describes the proposed numerical model; Chapter 3 details the dataset used for the calibration of the model; Chapter 4 presents the results of the calibration process. Finally, Chapter 5 reports some concluding considerations on the research work conducted.

TRANMPD-HM MODEL

Plastic transport was integrated into XBeach following an approach analogous to sediment dynamics. To incorporate non-buoyant plastics, a state-of-the-art review was here conducted to identify suitable methodologies for plastic transport simulation. The review focused on key aspects such as settling velocity, critical thresholds for incipient motion, and transport under combined wave and current effects.

Figure 1 provides a schematic overview of the key modifications implemented in XBeach to simulate the transport of plastic debris.

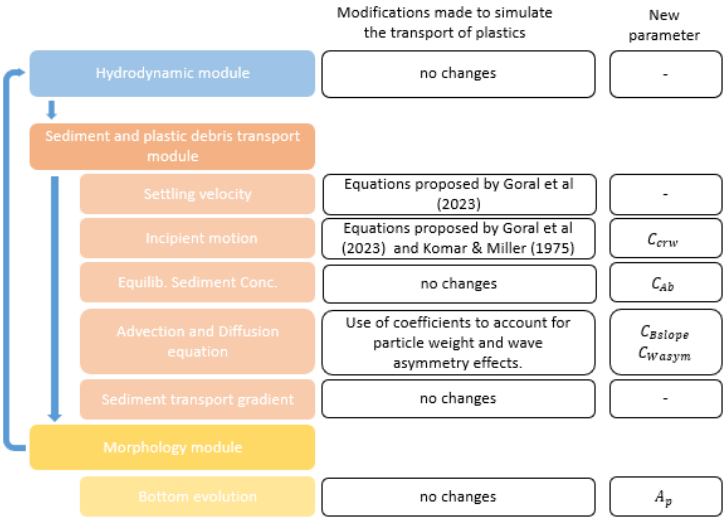

Figure 1: Schematic overview of Xbeach modifications.

Xbeach model

Xbeach features several key modules, including the hydrodynamic module, the sediment transport module, and the bottom evolution module, all of which were used in this study (see 1). The hydrodynamic module computes wave characteristics and other relevant quantities such as velocity and pressure, which are subsequently used in other modules. For this research, the surfbeat mode was applied to simulate wave properties. This mode solves short-wave motion using the wave action equation, which captures the behaviour of wave groups at a high level of detail. Additionally, the module incorporates wave-driven currents and undertow.

The sediment transport module in XBeach enables accurate simulations of sediment dynamics near the coast. Sediment concentrations within the water column are modeled using a depth-averaged advection-diffusion scheme, incorporating a source-sink term based on equilibrium sediment concentrations:

$$\frac{\partial hC}{\partial t} + \frac{\partial hC(u^E - u_a \sin\theta_m)}{\partial x} + \frac{\partial hC(v^E - u_a \cos\theta_m)}{\partial y} + \frac{\partial}{\partial x}\left[D_h h \frac{\partial C}{\partial x}\right] + \frac{\partial}{\partial y}\left[D_h h \frac{\partial C}{\partial y}\right] = \frac{hC_{eq} - hC}{T_s}, \quad (1)$$

where h is the local depth, C is the sediment concentration, t is time, u^E and v^E are the Eulerian velocity components, D_h is the diffusion coefficient, C_{eq} is the equilibrium concentration, θ_m is the wave incidence angle, and T_s is the particle response time. The term u_a represents the velocity component due to wave skewness and asymmetry, calculated as:

$$u_a = \gamma_{ua}(S_k + A_s)u_{rms}, \quad (2)$$

where S_k is the wave skewness, A_s is the wave asymmetry parameter, u_{rms} is the root-mean-square orbital velocity, and γ_{ua} is a calibration coefficient estimated using the relationship proposed by Elsayed and

Oumeraci (2017):

$$\gamma_{ua} = 5.93 s_s^{1.35}, \tag{3}$$

with s_s being the average slope steepness. The equilibrium concentration C_{eq} and adaptation time T_s depend on sediment properties. In this study, C_{eq} was estimated using the Soulsby-Van Rijn method (Soulsby, 1997), and T_s was calculated as:

$$T_s = \max\left(f_{Ts}\frac{h}{w_s}, T_{s,\min}\right), \tag{4}$$

where w_s is the sediment fall velocity, and f_{Ts} is a calibration factor. The term C_eq represents the equilibrium concentration, i.e., the amount of sediment transported due to current and waves. The transport formulations implemented in XBeach distinguish the transport of bottom load $C_{eq,b}$ and suspended load $C_{eq,s}$. There are various methodologies for estimating this term in Xbeach. In the present study, the Van Thiel-Van Rijn method was used (Van Rijn, 2007):

$$C_{eq,b} = \frac{A_{s,b}}{h}\left(\sqrt{v_{mg}^2 + 0.64 u_{rms,2}^2}\,) - U_{cr}\right)^{1.5} \tag{5}$$

where v_{mg} is the velocity magnitude, $u_{rms,2}$ is the adjusted orbital velocity to account for wave-breaking induced turbulence due to short waves (Van Thiel de Vries, 2009), $U_{cr}$is the critical velocity computed as a weighted summation of the separate contributions by currents (Shields, 1936) and waves (Komar and Miller, 1975), and $A_{s,b}$ is the bed-load coefficient calculated with:

$$A_{sb} = C_{Ab} h \frac{(D_{50}/h)^{1.2}}{(\Delta g\, D_{50})^{0.75}} \tag{6}$$

where D_{50} is the average grain diameter for all sediment classes.

Bed slope influences sediment transport in various ways (Walstra et al., 2007). The influence of bed slope on local hydrodynamics is not considered in XBeach. Two possible expressions were implemented to change the magnitude of sediment transport. The default method in XBeach is:

$$q_{x,slope} = q_x - \alpha h C \sqrt{(u^L)^2 + (v^L)^2}\frac{\partial z_b}{\partial x} \tag{7}$$

$$q_{y,slope} = q_y - \alpha h C \sqrt{(u^L)^2 + (v^L)^2}\frac{\partial z_b}{\partial y} \tag{8}$$

where q_x and q_y are the sediment transport rates in the x and y directions, C is the actual sediment concentration, u^L and v^L are the Lagrangian velocities, defined as the distance a water particle travels in one wave period, divided by that period and α is a calibration coefficient. Bed level changes are calculated based on sediment transport gradients using:

$$\frac{\partial z_b}{\partial t} + \frac{f_{mor}}{1-p}\left(\frac{\partial q_x}{\partial x} + \frac{\partial q_y}{\partial y}\right) = 0, \tag{9}$$

where z_b is the bed level, p is the porosity of the sediment, f_{mor} is the morphological acceleration factor, and q_x and q_y are the sediment transport rates in the x- and y-directions, respectively.

Changes introduced in Xbeach

For settling velocity, empirical equations were adopted, based on the work of Goral et al. (2023a), who analyzed 66 microplastic particles, and proposed formulas tailored to various shapes, including spherical, cylindrical and irregular geometries. The critical motion due to currents was evaluated using the Shields parameter method (Goral et al., 2023b), while the wave-induced motion was calculated using the method of Komar and Miller (1975), which is already implemented in XBeach.

The state-of-the-art analysis has not led to the identification of a method to predict plastic transport. Several studies have investigated this process for various types of plastics; however, these analyses have not resulted in the development of generalized empirical methods. To address this limitation, a calibration process was initiated making use of the model already present in Xbeach for sediments. The Xbeach code

was modified by introducing five additional calibration coefficients: A_p, which accounts for the fact that plastics have a transport velocity higher than that of sand; C_{crw}, which considers that the motion of plastics does not occur on a homogeneous mass but rather on a sand bed; C_{Ab}, which takes into account that plastics have different velocities; C_{slope}, which emphasizes the effect of gravity on plastic particles; and C_{Wasym}, which highlights the effects of wave asymmetry on transport.

The morphological acceleration factor (f_{mor}) speeds up the morphological time scale relative to the hydrodynamic timescale. In the same way, the parameter A_p speeds up the transport time of the plastic for morphological time:

$$f_p = A_p f_{mor} \tag{10}$$

where f_p is the acceleration factor of the plastic displacement.

In the modified version of Xbeach, the critical velocity ($U_{crw,e}$) due to the waves is estimated according to $U_{crw,e} = C_{crw} U_{crw}$ where U_{crw} is the value estimated by Xbeach with the method proposed by Komar and Miller (1975). The comparison of the movement of different types of plastics has shown that, under the same wave conditions, some plastics are transported at a much higher velocity than others. To account for this aspect, the coefficient C_{Ab} was introduced, which modifies the Van Thiel-Van Rijn equation based on the type of plastic:

$$A_{sb} = C_{Ab} h \frac{(D_{50}/h)^{1.2}}{(\Delta g D_{50})^{0.75}} \tag{11}$$

In relation to the seabed slope and the characteristics of plastics, the transport phenomenon can be predominantly influenced either by the particle weight or by wave asymmetry. To account for this aspect, two coefficients have been introduced C_{slope} and C_{Wasym}. The parameter C_{slope} was added to calibrate the relationship that accounts for the effect of the slope

$$q_{x,slope} = q_x - C_{slope} \alpha h C \sqrt{(u^L)^2 + (v^L)^2} \frac{\partial z_b}{\partial x} \tag{12}$$

$$q_{y,slope} = q_y - C_{slope} \alpha h C \sqrt{(u^L)^2 + (v^L)^2} \frac{\partial z_b}{\partial y} \tag{13}$$

while the parameter C_{Wasym} was introduced to amplify the effect of wave asymmetry

$$u_a = C_{Wasym}\, \gamma_{ua}\, (S_k - A_s)\, u_{rms} \tag{14}$$

CALIBRATION DATASET AND MODEL SETTING

The calibration process was carried out by replicating a laboratory transport experiment on plastics conducted by Guler et al. (2022), which focused on studying plastic transport in the nearshore zone. This experimental research investigates the cross-shore transport and accumulation of non-buoyant microplastic particles under irregular breaking waves on live sediment beds. The study examines two bed configurations in a wave flume: a plane bed and a pre-developed singly-barred profile, representing different stages of sediment morphology. A total of 18 microplastic particle groups with varying shapes, densities, and sizes were tested over extended durations, allowing the identification of four primary accumulation zones: offshore, the breaker bar, the plateau region, and the beach. The study highlights the importance of realistic initial bottom profiles, as these significantly affect transport patterns. In the barred profile runs, particles exhibited a complex behaviour, with offshore transport dominated by plunging waves at the breaker bar and onshore transport driven by wave-induced bed shear stresses. These observations highlight the need to consider detailed bottom morphologies and wave dynamics for accurate predictions of microplastic dispersion in coastal areas.

The verification of the computational code was conducted using results related to the dynamics of three types of plastic on the barred beach profile. Table 1 presents the key properties of the selected plastic particles. This manuscript focuses on the calibration processes for the sphere and rectangular cylinder, as the calibration for the cube has been detailed in Iuppa and Faraci (2024).

The experiments conducted by Guler et al. (2022) allowed for the evaluation of the average direction of plastic transport due to irregular wave motion. One of the most interesting findings is that plastic transport

Table 1: Plastic properties used in the study.

Plastic	Shape	Density [kg/m^3]	Size [mm]	Dean number [-]
POM	Sphere	1358	5	0.46
PLA	Cube	1187	5x5x5	0.84
PLA	Rectangular cylinder	1214	3x2x1	1.87

is influenced by the Dean number, defined as:

$$\Omega_p = \frac{H_{m0}}{T_p w_p} \tag{15}$$

where H_{m0} indicates the significant wave height; T_p indicates the peak wave period and w_p indicates the settling velocity of the particle. The Dean number represents the comparison between the energy carried by waves and the resistance of the sediment to movement.

Figure 2 shows the final distribution of the plastic debris for the three samples considered in our studies. The symbols N_p and $N_{p,t}$ represent the number of particles in each zone and the total number of particles used in the test, respectively. Particles with lower Ω_p (0.64) tended to migrate offshore or accumulate near the beach, while those with higher Ω_p (> 1.2) showed enhanced onshore accumulation at the plateau or beach zones. In the intermediate range of Ω_p, particles exhibited both onshore and offshore movement.

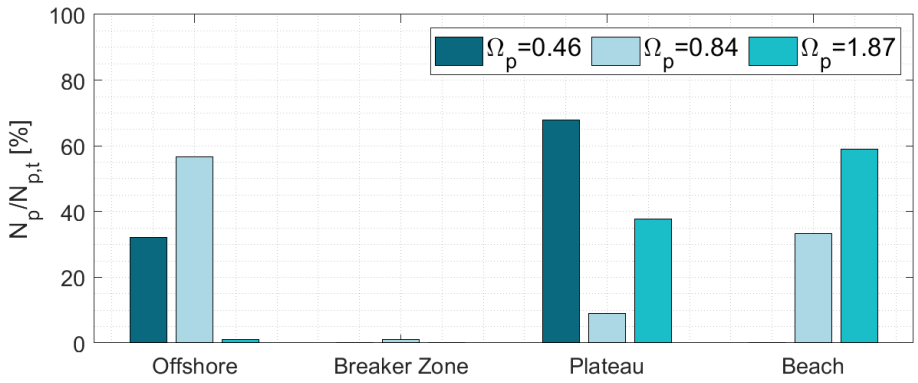

Figure 2: Final concentration of the plastic debris estimated by Guler et al. (2022). The correspondence between dean number and plastic is as follows: *i*) Ω_p=0.46 for the sphere; *ii*) Ω_p=0.84 for the cube; *iii*) Ω_p=1.87 for the rectangular cylinder.

Spherical particles, due to the low Dean number, tend to move offshore. In this case, their motion is primarily influenced by the weight of the particles. Once wave motion is initiated, a rapid displacement of the particles is observed, predominantly directed offshore. Specifically, a swift migration of the particles from the beach zone to the nearshore zone is noted, occurring within extremely short timeframes. Similar behaviour can be observed in the breaker zone, where the particles tend to move offshore. These results indicate that the transport is primarily influenced by the weight of the particles rather than by wave asymmetry. To emphasize this behaviour in TRANMPD-HM, the value of the C_{slope} was examined. A different behaviour is observed for rectangular cylinders. In this case, the particles show movement directed toward the beach. Here, the transport is primarily influenced by wave asymmetry. Consequently, the calibration process focused on defining the C_{Wasym}. In the case of cubes, the movement occurs both offshore and toward the beach. In this case, the calibration process carried out by Iuppa and Faraci (2024) was focused on both coefficients.

The characteristics of the plastic and the initial bottom configuration were provided to the modified version of XBeach as input. The plastic elements at the beginning of the simulation were placed in three different positions, following the same approach of Guler et al. (2022). At the beginning of the simulation, Guler et al. (2022) placed 90 plastic pieces equally distributed at three distinct points within the breaker zone, the plateau, and the beach zone respectively. The transportation of the plastic pieces was simulated

for approximately 84 hours using as input a wave with a spectral significant wave height (H_{m0}) of 0.16 m and a wave period (T) of 1.6 s. For each type of plastic, the five calibration coefficients were varied to identify the values that allow for an accurate reproduction of the experimental data.

The concentration of plastics was analysed by considering the four zones indicated in Figure 3, following Guler et al. (2022).

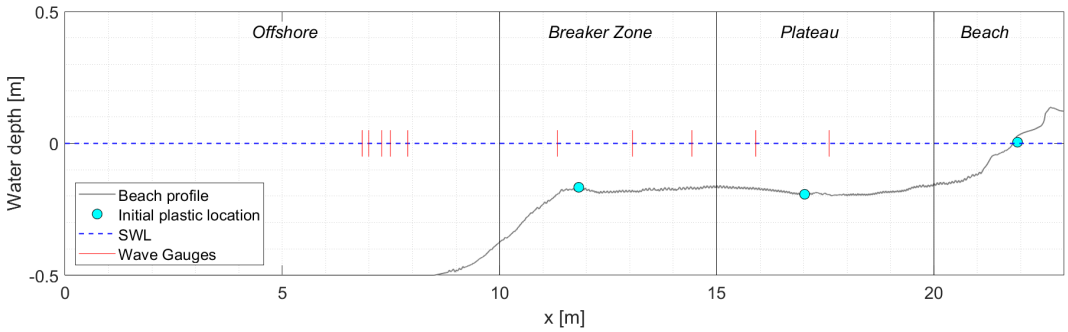

Figure 3: Cross-section of the beach used in the experiments of Guler et al. (2022) and implemented in the numerical model.

Table 2 shows the main input of TRANMPD-HM (wave, sediment characteristics and main numerical model setting).

Table 2: The main input provided to TRANMPD-HM: wave, sediment characteristics and main numerical model setting.

Name	Symbol	Value
Wave height	H_{m0}	0.16 m
Wave period	T	1.6 s
Simulation duration	t_{tot}	84 hours
Spectrum	–	JONSWAP
Computational cell size	Δ_x	1 cm
Total number of particles	$N_{p,t}$	90
Location of release points	$N_{p,t}$	11.8, 17.0, 21.9 m
Median diameter sediment	D_{50}	0.18 mm
Density of the sediments	ρ_s	2650 kg/m^3
Sediment settling velocity	w_s	0.124 m/s
Sediment Dean number	Ω_p	6.00
Calibration factor	γ_{ua}	0.20
Equilibrium concentration	C_{eq}	Soulsby-Van Rijn

RESULTS

The comparison between the experimental data and the numerical model data focused on the hydrodynamic module and plastic transport. Specifically, regarding the first aspect, reference was made to the wave height.

Figure 4 presents a comparison between the root-mean-square wave height (H_{rms}) obtained from the measurements by Guler et al. (2022) and the values predicted by the numerical model. During the experimental campaign, measurements of wave characteristics were taken at different positions within the channel (see Figure 3). The analysis of the measurements shows almost identical values for the probes placed in the offshore zone, while for the probes located beyond the breaking zone, a gradual decrease in wave height is observed. The data comparison shows a good correspondence between the estimated values and the experimental ones. The mean absolute difference is equal to 0.018 m.

For each type of plastic, the five calibration coefficients were varied to identify the values that allow an accurate reproduction of the experimental data. In particular, with regard to the coefficients A_p and C_{crw},

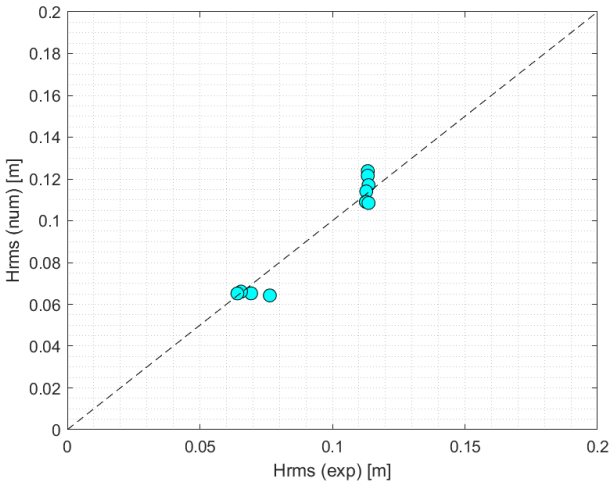

Figure 4: Comparison between the wave height measured by Guler et al. (2022) and that estimated by the numerical model.

reference was made to the study conducted by Iuppa and Faraci (2024). In such a study, it was found that to account for the velocity of plastic movement relative to sediments, a value of A_p equal to 100,000 should be considered. For the incipient motion condition, the best correspondence is observed for C_{crw} equal to 0.1.

Figure 5 and Figure 6 show the comparison between the concentration of the plastic debris measured by Guler et al. (2022) and that estimated by the numerical model. The concentration is obtained considering different values of the calibration coefficients. In the calibration process, numerous configurations obtained by varying the values of the calibration coefficients were considered; those reported in the figures represent a selection of the most significant ones for the present study. In some cases, the simulation was halted because the results showed substantial discrepancies compared to the experimental data.

For the sphere (Ω_p = 0.46) the coefficient value C_{Wasym} was set equal to 0 since transport is mainly affected by the weight of the particles. For C_{slope}=1 the transport of particles occurs at velocities that are not consistent with those observed in experiments (see Figure 5, first row). For C_{slope}=2, the concentration seems more similar to that observed (see Figure 5, second row). However, at a certain moment, the plastic in the nearshore zone tends to move offshore. The best match is observed for C_{slope}=3. In this case, the evolution of the concentration aligns with the observed timing (see Figure 5, third row).

For the rectangular cylinder (Ω_p=1.87) the value of the coefficient C_{slope} was set equal to 0 since the transport is mainly affected by the wave asymmetry. For C_{Ab}=0.015 and C_{Wasym}=2, the plastics are not transported to zones other than their release. The increase in the C_{Ab} to 2 results in transport that still differs from that observed in the experiments (see Figure 6, second row). For C_{Wasym} = 2, in the break zone, the concentration variation estimated by the numerical model closely matches that observed in the physical model. However, in other zones, the concentration is overestimated. The behaviour of the experimental data appears unusual, as particles positioned in the nearshore zone are transported toward the beach a few minutes after the test begins. For particles originating from the breaker zone, the transport velocity significantly decreases. The evolution of the seabed might explain this behavior. In the experimental tests, plastic motion is studied concurrently with seabed evolution. Therefore, the anomaly could be attributed to changes in the seabed, which caused a deceleration of particles coming from the breaker zone. Unfortunately, data on seabed evolution is unavailable, making it impossible to verify this aspect numerically. This result highlights the necessity of accounting for morphodynamic processes occurring during the transport process in future applications.

The calibration process allowed the identification of the coefficients listed in Table 3.

CONCLUSIONS

This study focused on developing and validating a numerical model designed to predict the transport of non-buoyant plastic debris in coastal zones, addressing a pressing environmental challenge. Integrat-

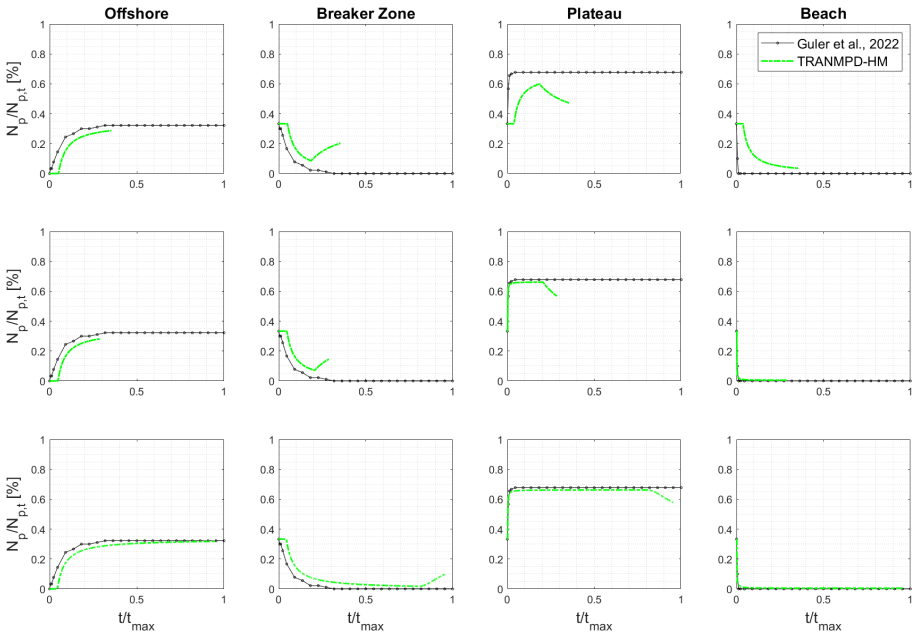

Figure 5: Comparison between the concentration of the plastic debris measured by Guler et al. (2022) and that estimated by the numerical model. The results are related to the sphere ($\Omega_p = 0.46$). Values of the coefficients: first row C_{Ab}=0.015, C_{slope}=1, and C_{Wasym}=0; second row C_{Ab}=0.015, C_{slope}=2, and C_{Wasym}=0; third row C_{Ab}=0.015, C_{slope}=3, and C_{Wasym}=0.

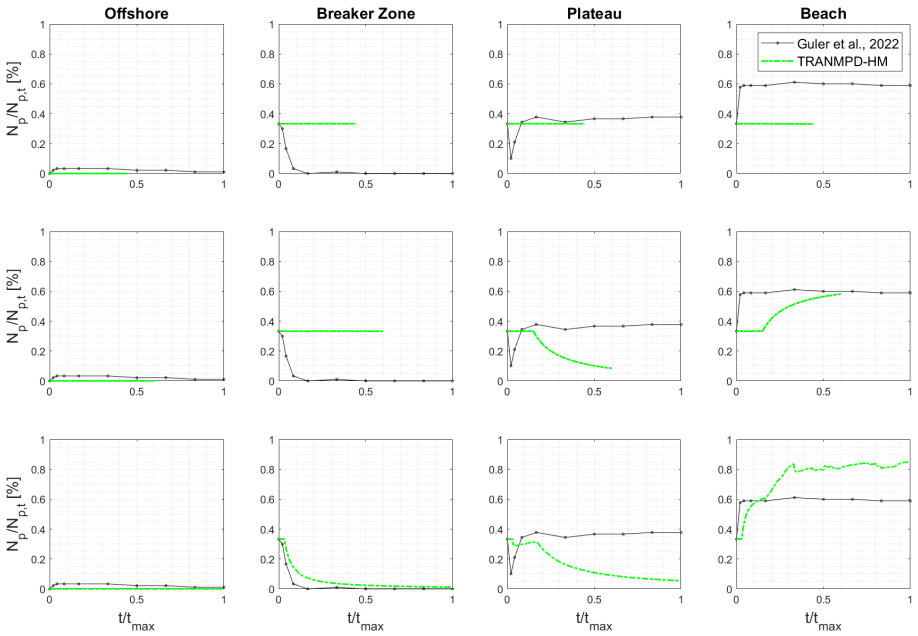

Figure 6: Comparison between the concentration of the plastic debris measured by Guler et al. (2022) and that estimated by the numerical model. The results are related to the rectangular cylinde ($\Omega_p = 1.87$). Values of the coefficients: first row C_{Ab}=0.015, C_{slope}=0, and C_{Wasym}=2; second row C_{Ab}=2, C_{slope}=0, and C_{Wasym}=2; third row C_{Ab}=2, C_{slope}=0, and C_{Wasym}=4.

ing empirical models into the modified Xbeach code enabled the estimation of critical transport parameters, enhancing the model's capacity to simulate the complex interplay between hydrodynamics, sediment transport, and plastic dynamics. A significant contribution of this research was the introduction of five

Table 3: Plastic properties and calibration coefficients.

Plastic	**Shape**	A_p	C_{crw}	C_{Ab}	C_{slope}	C_{Wasym}
POM	Sphere	100,000	0.1	0.015	3	0
PLA	Cube	100,000	0.1	0.015	1	1
PLA	Rectangular cylinder	100,000	0.1	2	0	4

calibration coefficients, which facilitated a more accurate representation of plastic behaviour under diverse hydrodynamic conditions. These parameters allowed the model to replicate experimental observations, demonstrating its effectiveness in capturing the dynamics of plastic transport. Future research will focus on refining these calibration parameters to further optimize the model and enhance its predictive accuracy, particularly in scenarios involving simultaneous seabed evolution.

ACKNOWLEDGEMENTS

This research has been funded by the European Union - Next Generation EU, Mission 4 Component 1 - CUP J53D23019300001 (PRIN PNRR2022 P2022S2WJZ ManagIng plastic traNspOrt in riverS and coaStal arEas, MINOSSE).

References

J. M. Alsina, C. E. Jongedijk, and E. van Sebille. Laboratory measurements of the wave-induced motion of plastic particles: Influence of wave period, plastic size and plastic density. *Journal of Geophysical Research: Oceans*, 125(12):e2020JC016294, 2020.

S. M. Elsayed and H. Oumeraci. Effect of beach slope and grain-stabilization on coastal sediment transport: An attempt to overcome the erosion overestimation by xbeach. *Coastal Engineering*, 121:179–196, 2017.

P. L. Forsberg, D. Sous, A. Stocchino, and R. Chemin. Behaviour of plastic litter in nearshore waters: First insights from wind and wave laboratory experiments. *Marine Pollution Bulletin*, 153:111023, 2020.

K. D. Goral, H. G. Guler, B. E. Larsen, S. Carstensen, E. D. Christensen, N. B. Kerpen, T. Schlurmann, and D. R. Fuhrman. Settling velocity of microplastic particles having regular and irregular shapes. *Environmental Research*, 228:115783, 2023a.

K. D. Goral, H. G. Guler, B. E. Larsen, S. Carstensen, E. D. Christensen, N. B. Kerpen, T. Schlurmann, and D. R. Fuhrman. Shields diagram and the incipient motion of microplastic particles. *Environmental Science & Technology*, 57(25):9362–9375, 2023b.

F. Guerrini, L. Mari, and R. Casagrandi. The dynamics of microplastics and associated contaminants: Data-driven lagrangian and eulerian modelling approaches in the mediterranean sea. *Science of The Total Environment*, 777:145944, 2021. ISSN 0048-9697. doi: https://doi.org/10.1016/j.scitotenv.2021.145944. URL `https://www.sciencedirect.com/science/article/pii/S0048969721010111`.

H. G. Guler, B. E. Larsen, O. Quintana, K. D. Goral, S. Carstensen, E. D. Christensen, N. B. Kerpen, T. Schlurmann, and D. R. Fuhrman. Experimental study of non-buoyant microplastic transport beneath breaking irregular waves on a live sediment bed. *Marine Pollution Bulletin*, 181:113902, 2022.

C. Iuppa and C. Faraci. A numerical tool for non-buoyant plastic debris short-term fate prediction in the nearshore zone. In *2024 IEEE International Workshop on Metrology for the Sea; Learning to Measure Sea Health Parameters (MetroSea)*, pages 369–374. IEEE, 2024.

C. Iuppa, G. Passalacqua, and C. Faraci. An equilibrium criterion for plastic debris fate in wave-driven transport. *Marine Pollution Bulletin*, 206:116758, 2024.

P. D. Komar and M. C. Miller. Sediment threshold under oscillatory waves. *Coastal Engineering 1974*, pages 756–775, 1975.

S. Liubartseva, G. Coppini, R. Lecci, and E. Clementi. Tracking plastics in the mediterranean: 2d lagrangian model. *Marine Pollution Bulletin*, 129(1):151–162, 2018. ISSN 0025-326X. doi: https://doi.org/10.1016/j.marpolbul.2018.02.019. URL https://www.sciencedirect.com/science/article/pii/S0025326X18301000.

P. Núñez, A. Romano, J. García-Alba, G. Besio, and R. Medina. Wave-induced cross-shore distribution of different densities, shapes, and sizes of plastic debris in coastal environments: A laboratory experiment. *Marine Pollution Bulletin*, 187:114561, 2023.

D. Roelvink, R. McCall, S. Mehvar, K. Nederhoff, and A. Dastgheib. Improving predictions of swash dynamics in xbeach: The role of groupiness and incident-band runup. *Coastal Engineering*, 134:103–123, 2018.

A. Shields. Anwendung der aehnlichkeitsmechanik und der turbulenzforschung auf die geschiebebewegung. *PhD Thesis Technical University Berlin*, 1936.

R. Soulsby. Dynamics of marine sands. 1997.

L. C. Van Rijn. Unified view of sediment transport by currents and waves. ii: Suspended transport. *Journal of hydraulic Engineering*, 133(6):668–689, 2007.

J. Van Thiel de Vries. Dune erosion during storm surges. 2009.

D. Walstra, L. Van Rijn, M. Van Ormondt, C. Brière, and A. Talmon. The effects of bed slope and wave skewness on sediment transport and morphology. In *Coastal Sediments' 07*, pages 137–150. 2007.